ELSEVIER

International Journal of Mass Spectrometry 185/186/187 (1999) 75–90

International Journal of Mass Spectrometry

Partitioning of kinetic energy to internal energy in the low energy collision-induced dissociations of proton-bound dimers of polypeptides

Guodong Chen[a], R. Graham Cooks[a,*], David M. Bunk[b], Michael J. Welch[b], John R. Christie[c]

[a]*Department of Chemistry, Purdue University, West Lafayette, IN 47907-1393, USA*
[b]*Analytical Chemistry Division, Chemical Science and Technology Laboratory, National Institute of Standards and Technology, Gaithersburg, MD 20899, USA*
[c]*School of Chemistry, La Trobe University, Bundoora, Victoria 3083, Australia*

Received 23 April 1998; accepted 3 July 1998

Abstract

Collision-induced dissociation (CID) of the proton-bound dimers of a set of pentapeptides (leucine enkephalin analogs) generated by electrospray ionization is studied as a function of collision energy under conditions of single collisions with argon. As the collision energy is increased, the abundances of the two protonated peptides become more similar, indicating an increase in internal energy deposition. The effective temperature (T_{eff}) of the cluster ions is calculated by the kinetic method and found to increase approximately linearly with collision energy. Knowing the fragmentation thermochemistry, the ion internal energy is characterized using the kinetic method. The partitioning quotient for the conversion of laboratory kinetic energy into internal energy for these cluster ions is 2% to 5% in the 50 eV to 200 eV collision energy range. Average relative standard deviations of multiple measurements of partitioning quotients are around 15% and are mainly due to uncertainties in ion abundance ratios. Unimolecular dissociation Rice–Ramsperger–Kassel–Marcus (RRKM) theory is used to calculate the relationship between the fragment ion abundance ratio and the total internal energy of the cluster ions. Comparison of these data with experiment allows the energy partitioning behavior to be characterized independently and more accurately. The partitioning quotient obtained in this way ranges from 2 ± 1.0% (uncertainty is the standard derivation of multiple measurements) to 5 ± 1.0%. These data are consistent with either an impulsive collisional activation mechanism or with collision complex formation. (Int J Mass Spectrom 185/186/187 (1999) 75–90) © 1999 Elsevier Science B.V.

Keywords: Energy partitioning; Proton-bound dimers; Kinetic method; Peptide dissociation

1. Introduction

The activation and dissociation of biological molecular ions in the gas phase and their intrinsic thermochemical properties are subjects of growing interest. Research in this area has been greatly facilitated by the development of the technique of electrospray ionization (ESI) [1, 2]. Typical of this type of inquiry have been investigations by a number of groups into the phenomenon of large energy loss during collision-induced dissociation (CID) of peptide ions [3–5] and its explanation in terms of impulsive collisions [6, 7] and target atom excitation [8]. In a

* Corresponding author.

Dedicated to Professor M.T. Bowers on the occasion of his 60th birthday, and in appreciation of his leading role in the field of mass spectrometry.

PII S1387-3806(98)14078-2

study of the unimolecular decomposition kinetics of multiply protonated melittin molecular ions in different charge states, Smith et al. [9] found differences in the estimated activation energies for the reactions of the different charge states and ascribed them to the destabilizing effects of coulombic repulsion in highly charged ions. However, greater stability in higher charged state ions has been observed in some other cases, for example, Williams et al. found that activation energies for 10+ and 11+ ubiquitin ions are 1.6 eV, although activation energies for 6+ and 7+ ions are 0.9–1.0 eV [10]. In a related study, Wysocki et al. [11] compared unimolecular decompositions of protonated peptides and peptide dimers by thermal and surface-induced dissociation (SID) and estimated the effective temperatures (a measure of the internal energy) of activated protonated peptide ions and their symmetrical dimers from the SID data. They also estimated the average activation energies of low-energy fragmentation processes of protonated oligopeptides by using ESI/SID data in combination with RRKM (Rice–Ramsperger–Kassel–Marcus) theory and found a value of (1.56 ± 0.22) eV for the lowest energy fragmentation of protonated leucine enkephalin [12]. Williams and co-workers [10, 13, 14], using the relatively new procedure of blackbody infrared radiative dissociation (BIRD), measured the activation energies and entropies of thermal dissociations of ionized biomolecules. The Arrhenius activation energies for dissociation of proton-bound homodimers of N,N-dimethylacetamide, glycine, alanine, and lysine, and the heterodimer alanine/glycine were obtained by this technique, and the binding energies of the proton-bound amino-acid dimers were found to fall in the narrow range of 1.15 ± 0.05 eV [15]. Other studies have provided evidence for internal salt bridges in some protonated peptides and suggested the possibility of inter-molecular binding through salt bridges in some of their proton-bound dimers [14, 16]. Williams et al. found that higher binding energies (~1.4 eV) are associated with the ion-zwitterion rather than the proton-bound structures of protonated base/betaine complexes [17].

There is a substantial literature on the kinematics of collisional activation for small polyatomic ions including experiments at both high and low collision energies [18], experiments performed as a function of scattering angle [19–21], and experiments in which the target is a surface rather than a gaseous atom or molecule [22]. Partitioning of translational into internal energy occurs during collisional activation and the amount of energy interconverted can provide, at least in principle, information on the mechanism of collisional activation. At low relative velocities, collision-induced dissociation may proceed by the formation of a collision complex [23], although this process is not well characterized. The energy transfer in low energy CID is often quite high, partly because of the usual use of multiple collision conditions. Single collisions at low collision energies deposit a relatively broad range of internal energies [24, 25] and the energy partitioning quotient ($T \rightarrow V$) is 15 ± 5% of the center of mass energy for several ions and a number of targets [26]. For collisions in the keV energy range, the internal energy deposited covers an even wider range and increasingly endothermic dissociation channels are accessed by those low probability collision events that are associated with larger $T \rightarrow V$ conversion efficiencies [27].

Given the situation for small ions, it may not be surprising that there is virtually no information available on the topic of energy partitioning in the activation of biomolecules. Marzluff et al. [28, 29] reported that low energy CID of deprotonated polypeptides at a laboratory energy in the range of 50 eV displays a center of mass $T \rightarrow V$ conversion efficiency of 55 % for tripeptides and trajectory calculations suggested more than 90% efficiency for protonated nonapeptide bradykinin under single-collision conditions. Boyd and co-workers [7, 30–32] also studied the CID of protonated peptides and evaluated the relative kinetic energy to internal energy conversion from the ion abundance ratios of selected fragment ions with known energy requirements. Their results indicate that a simple momentum transfer mechanism of collisional activation operates for small organic precursor ions although the binary (impulsive) model becomes dominant as the precursor mass is increased. In the experiments described below, kinetic energy to internal energy conversion for proton-bound dimers

of polypeptides is estimated by the kinetic method and the implications of the results for the mechanism of collisional activation are explored.

The kinetic method is an approximate method that is normally used to make thermochemical determinations based on the rates of competitive dissociations of mass-selected cluster ions [33, 34]. However, it can also be used to characterize the energy of the activated cluster ion in cases where the thermochemical data is already known. In the case of proton-bound dimers, the fragmentation of the mass-selected proton-bound dimers to give the individual protonated bases can be expressed by Eq. (1).

$$\begin{array}{lll} & k_1 & AH^+ + B \\ A{-}H^+{-}B & \nearrow\ \ \searrow & \\ & k_2 & A + BH^+ \end{array} \qquad (1)$$

The ratio of the rates of the competitive dissociations of the proton-bound dimer, expressed as the ratio of the abundances of the individual protonated bases, can be used to determine the proton affinity difference between the two monomers [Eq. (2)]. Theoretical treatments of the kinetic method, given elsewhere, lead to the following approximate relationship [35–39]:

$$\ln([AH^+]/[BH^+]) = \Delta GB/(RT_{\text{eff}}) \qquad (2)$$

In Eq. (2), $[AH^+]$ and $[BH^+]$ are the abundances of the two protonated bases, ΔGB is the difference in gas-phase basicities of compounds A and B, and T_{eff} is the effective temperature of the activated dimer ion. As discussed by Vékey [40], the effective temperature is the temperature of a population of ions that has a Boltzmann distribution of internal energies such that the same fragment ion abundances are observed as in the non-Boltzmann ion population being studied. The kinetic method has previously been used to examine the internal energy deposition into proton-bound dimers upon CID [34, 41]. This follows from the fact that the effective temperature of the cluster ion can be estimated from Eq. (2), using dimeric ions comprised of compounds of known affinities. This approach provides an alternative to the use of small thermometer ions [24, 26, 42–44] for the estimation of internal energy deposition. Such an alternative is invaluable in cases where the traditional thermometer ion method is not applicable and this is the case for biomolecular ions generated by electrospray ionization.

While no previous attempts have been made to investigate the transfer of kinetic energy to internal energy in collisional activation of biological cluster ions, McLuckey [41] has demonstrated the possibility of using the kinetic method to obtain such information in simple amine systems, i.e. proton-bound dimers of amines. The collision energy dependence of the fragment ion abundance ratio was measured for proton-bound dimers of amines and RRKM calculations were used to estimate the total internal energy of the activated cluster ions [41]. The maximum average internal energy of the activated cluster ions was found to be ~4.3 eV at a laboratory collision energy of ~70 eV [41]. Assuming negligible initial internal energy, the energy partitioning quotient is ca. 6% of the lab collision energy, although a mechanism of collisional activation was not suggested. Similar measurements were later made in this laboratory [45].

In this article, we extend this approach and employ the kinetic method to study the collision energy dependence of proton-bound dimers comprised of model polypeptides (leucine enkephalin analogs). The proton-bound dimers were generated by electrospray ionization and subjected to CID under single collision conditions. The fragment ion abundance ratios were measured as a function of collision energy. Knowing the activation energies for the competitive dissociations, the effective temperature of the activated proton-bound dimers was calculated using the kinetic method. It was then straightforward to use this value to estimate the internal energy of the activated ion. Lee and Beauchamp [46] and Craig et al. [47] have both demonstrated from the RRK and RRKM theory that the effective temperature is a measure of the average internal energy in excess of the critical energy for dissociation per degree of freedom in the activated cluster ion. Recently, Vékey [40] has suggested the relationship shown in Eq. (3) between the effective temperature and the average value of the internal energy:

$$E_{\text{int}} = c(T, \nu)skT_{\text{eff}} \quad (3)$$

In this expression, s is the number of oscillators, k is the Boltzmann constant, T_{eff} is the effective temperature, and $c(T, \nu)$ is a temperature and frequency dependent factor with a value of ~0.2 in organic molecules at temperatures between 300 K and 450 K. The partitioning of kinetic energy in the laboratory frame of reference into internal energy can be estimated therefore using Eq. (4):

$$\rho_{T\equiv V} = [c(T, \nu)skT_{\text{eff}}]/KE \quad (4)$$

Differential measurements (in terms of collision energy) are preferred since they correct for the internal energy of the cluster ion before collision and minimize experimental errors. Hence we obtain Eq. (5) which was used to measure the energy partitioning quotient:

$$\rho_{T\equiv V} = [c(T, \nu)sk\Delta T_{\text{eff}}]/\Delta KE \quad (5)$$

The fragmentation data recorded in this study were also used in a different way to provide information on energy partitioning. The ratio of the rate constants for the competitive dissociation reactions was calculated as a function of internal energy by both RRK and RRKM theory. This information on fragmentation behavior as a function of the internal energy of the proton-bound dimers was combined with the fragment ion abundance ratios measured as a function of collision energy to provide an auxiliary (but not completely independent) estimate of the kinetic energy to internal energy conversion quotient.

2. Experimental

All experiments were performed using a Finnigan TSQ-70 triple quadrupole mass spectrometer (Finnigan MAT, San Jose, CA) fitted with an electrospray ionization source (Analytica, Branford, CT). Each sample was prepared from a mixture of two pentapeptides (leucine enkephalin analogs) dissolved in a suitable solvent (0.05% trifluoroacetic acid in 50% H_2O and 50% acetonitrile). The concentration was about 0.5 g/L for each pentapeptide. The sample solution was injected into the ion source at a flow rate of 1 μL/min using a syringe pump (Harvard Apparatus, Model 55-2222, South Natick, MA). The liquid sample flowed through a grounded needle at atmospheric pressure and was electrosprayed across a 4 kV potential through a counter-flow of heated (220 °C) nitrogen gas. The skimmer voltage was held at 200 V.

The proton-bound dimers generated in the electrospray ion source were mass-selected using the first quadrupole. Collisional activation of the dimer was achieved in the second quadrupole under single collision conditions, using an argon target gas at a pressure intended to achieve a main beam attenuation of 15% or less. The abundances of the fragment ions were measured as a function of collision energy from the product ion mass spectrum generated by scanning the third quadrupole. Multiple measurements were made for each fragment ion ratio. Typically, uncertainties in the fragment ion ratios decreased from 25% at low collision energy (10–50 eV) to 15% at high collision energy (50–200 eV). These uncertainties are propagated in the subsequent calculations of energy partitioning.

Leucine enkephalin (YGGFL) was commercially available and used as received (Sigma Chemical Co., St. Louis, MO). The four leucine enkephalin analogs (GGGFL, VGGFL, KGGFL, RGGFL) were synthesized at the Purdue Cancer Center (Purdue University, West Lafayette, IN). The identities and purities of the synthetic peptides were confirmed by high-performance liquid chromatography (HPLC) and electrospray ionization mass spectrometry (ESI-MS). Tandem mass spectrometry (MS/MS) further confirmed the structures of synthetic peptides.

3. Results and discussion

3.1. Proton-bound dimer formation and dissociation

Proton-bound dimers of pentapeptides were generated by electrospray ionization of binary peptide mixtures. Fig. 1 shows a typical mass spectrum of a mixture of two pentapeptides, KGGFL and YGGFL. In addition to the protonated monomers ($KGGFLH^+$

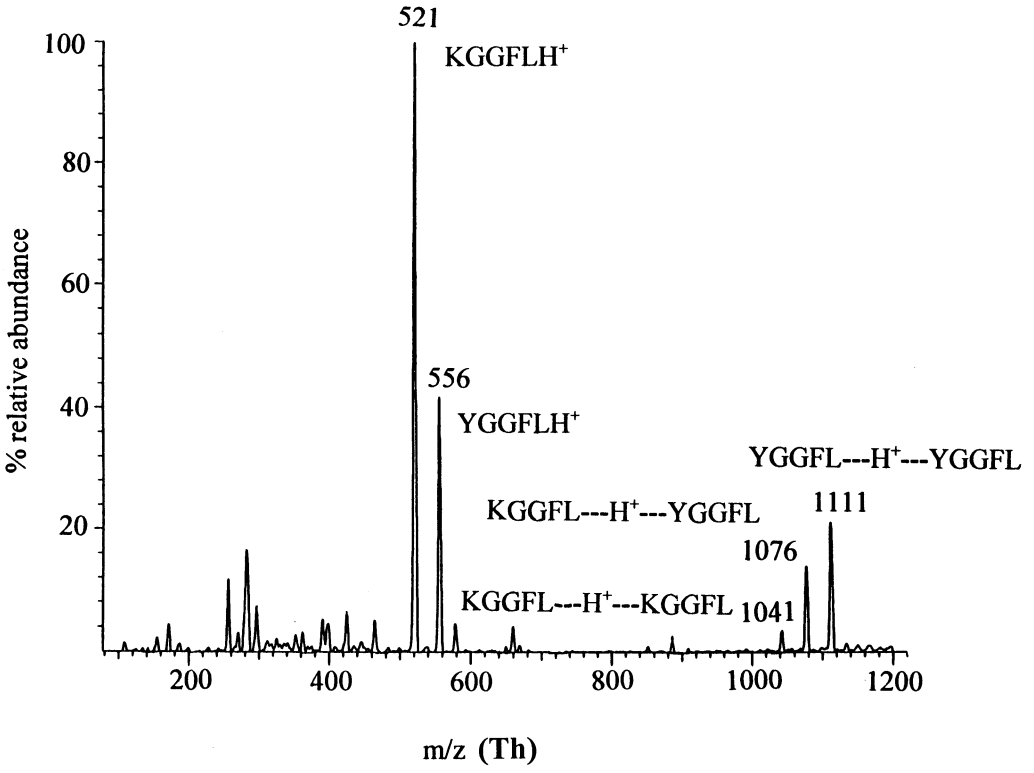

Fig. 1. Electrospray ionization mass spectrum of a pentapeptide mixture containing YGGFL and KGGFL.

and $YGGFLH^+$), all three proton-bound dimers are observed. As expected, CID of the heterodimer (KGGFL---H^+---YGGFL) at 1076 Thomson [Thomson (Th) = Da/charge] [48] produces just two fragment ions (Fig. 2), that are a result of the products of the two competing dissociations shown in Eq. (1). The product ions, at 521 Th and 556 Th, correspond to protonated KGGFL and protonated YGGFL, respectively. The ratio of the product ion abundances clearly indicates that KGGFL has a significantly greater *GB* than YGGFL. This is expected in view of the individual proton affinities of tyrosine (*Y*, PA = 220.2 kcal mol^{-1}) and lysine (*K*, PA = 227.2 kcal mol^{-1}) [34], which are the only different amino acid residues in the two pentapeptides. The product ion mass spectrum for this dimer is typical of the MS/MS product ion spectra recorded for other proton-bound dimer ions in this study.

In order to establish the relative GB's of all five pentapeptides, all combinations of proton-bound dimers of the pentapeptides were studied. Table 1 summarizes the CID results at 40 eV collision energy. As can be seen, the *GB*'s of the five pentapeptides are ordered as: RGGFL > KGGFL > YGGFL > VGGFL > GGGFL. This is consistent with the expectation that the *GB* of a small polypeptide is controlled by the PA of its most basic residue [34, 49]. For example, the *GB* of GGR (242.6 kcal mol^{-1}) is larger than the *GB* of GGL (217.2 kcal mol^{-1}), largely because of the different *PA*'s of argine (*R*, PA = 239.1 kcal mol^{-1}) and leucine (*L*, PA = 217.6 kcal mol^{-1}) [49]. The internal consistency of the data can be seen, for example, in the last three entries in Table 1, which allow a comparison of the measured value VGGFL/GGGFL of 2.5:1, with a predicted value of 4.6:1. However, there is an inconsistency in the case of KGGFL/YGGFL and KGGFL/VGGFL in which the predicted value YGGFL/VGGFL is 0.2, far different from the measured ratio (1.4:1). These errors are largest if data are confined to a single collision energy and they

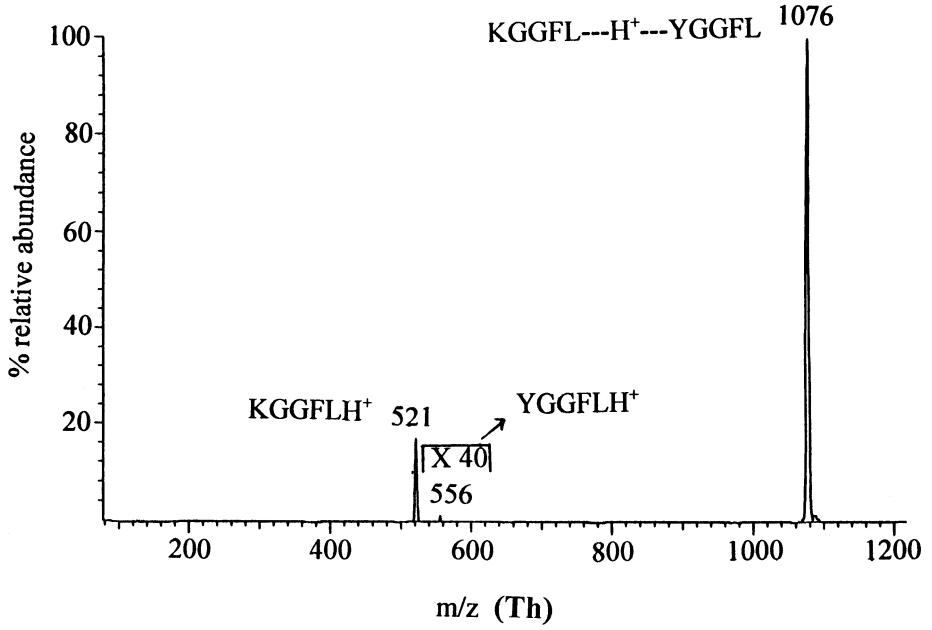

Fig. 2. Product ion MS/MS spectrum of the mass-selected proton-bound dimer composed of YGGFL and KGGFL (*m*/*z* 1076). Activation was achieved with 10 eV collision energy on an argon target gas under single collision conditions.

Table 1
CID of pentapeptide cluster ions (40 eV collision energy)

Peptide/peptide	Fragments of CID[a]	Gas phase basicity of peptide
RGGFL/KGGFL (*m*/*z* 1069)[b]	Two fragment ions (94:1)	GB(RGGFL) > GB(KGGFL)
RGGFL/YGGFL (*m*/*z* 1104)	One fragment ion (100:0)	GB(RGGFL) > GB(YGGFL)
RGGFL/VGGFL (*m*/*z* 1040)	One fragment ion (100:0)	GB(RGGFL) > GB(VGGFL)
RGGFL/GGGFL (*m*/*z* 998)	One fragment ion (100:0)	GB(RGGFL) > GB(GGGFL)
KGGFL/YGGFL (*m*/*z* 1076)	Two fragment ions (88:1)	GB(KGGFL) > GB(YGGFL)
KGGFL/VGGFL (*m*/*z* 1012)	Two fragment ions (18:1)	GB(KGGFL) > GB(VGGFL)
KGGFL/GGGFL (*m*/*z* 970)	Two fragment ions (133:1)	GB(KGGFL) > GB(GGGFL)
YGGFL/VGGFL (*m*/*z* 1047)	Two fragment ions (1.4:1)	GB(YGGFL) > GB(VGGFL)
YGGFL/GGGFL (*m*/*z* 1005)	Two fragment ions (6.4:1)	GB(YGGFL) > GB(GGGFL)
VGGFL/GGGFL (*m*/*z* 941)	Two fragment ions (2.5:1)	GB(VGGFL) > GB(GGGFL)

[a]The number in parentheses indicates the relative abundances of two fragment ions at 40 eV collision energy. See text for uncertainties.

[b]Mass/charge ratio of the proton-bound dimer.

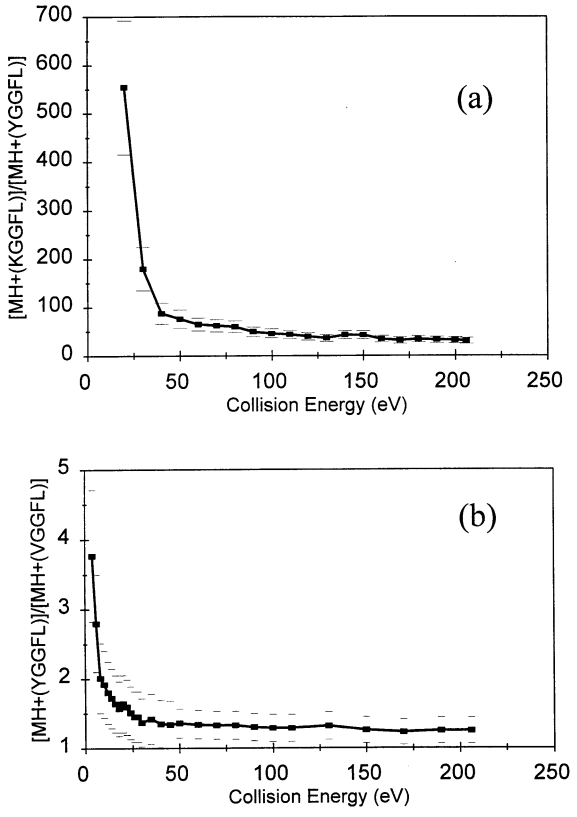

Fig. 3. Fragment ion ratios (a) $[MH^+(KGGFL)]/[MH^+(YGGFL)]$ and (b) $[MH^+(YGGFL)]/[MH^+(VGGFL)]$ vs. collision energies under single collision conditions. The error bars are estimated standard derivations of peak ratios.

would then produce relatively large uncertainties in the final energy partitioning measurements.

The collision energy dependence of the dissociation behavior of the proton-bound dimers was studied in an attempt to reduce the uncertainties and obtain additional information on the internal energy deposition. Fig. 3 displays the collision energy dependence for dissociation of KGGFL–H^+–YGGFL and YGGFL–H^+–VGGFL. The target gas pressure corresponds to single collisions and there is no secondary fragmentation. The effect of collision pressure was investigated in the case of KGGFL–H^+–YGGFL by making measurements at two different pressures, nominally 0.10 mTorr and 0.20 mTorr, corresponding to main beam attenuation of 10% and 15%. The data are identical, within experimental error, supporting the claim that single collision conditions are employed. It is evident from Fig. 3 that the fragment ion abundance ratio, which corresponds to the ratios of rate constants [k_1/k_2, Eq. (1)], decreases with increasing collision energy. This is consistent with calculations as well as previous studies on small proton-bound dimers where similar collision energy dependences were observed [36, 41, 45, 50]. A study on proton-bound dimers of peptides by Fenselau and co-workers [51] also revealed such a collision energy dependence for dimers generated by fast atom bombardment. Measurements on other proton-bound dimers, including RGGFL/KGGFL and VGGFL/GGGFL, show qualitatively similar collision energy dependences.

3.2. Estimation of kinetic energy to internal energy partitioning by the kinetic method

The effective temperature of the proton-bound dimers can be calculated from Eq. (2) if the fragment ion abundance ratio is measured and the difference in *GB*'s for the constituent peptides is known. Since the exact difference in *GB*'s for the pentapeptide pairs studied is not known, we assume that the difference in *GB*'s is mainly caused by the difference in the *GB*'s (and hence *PA*'s) of the most basic residue in the constituent peptides. This assumption is supported by previous studies by Wu and Fenselau [49] in which the basicities of a set of related peptides were ordered and found to show increments that correspond to the proton affinities of the most basic amino acids present in each. This result allows one to assume that ΔGB(RGGFL/KGGFL) = ΔPA(arginine/lysine), ΔGB(KGGFL/YGGFL) = ΔPA(lysine/tyrosine), ΔGB(YGGFL/VGGFL) = ΔPA(tyrosine/valine), and ΔGB(VGGFL/GGGFL) = ΔPA(valine/glycine). However, we recognize that this may not be true in cases where the structures of the proton-bound dimers are different. For example, salt-bridge binding observed in some cases by Price et al. affects the binding energies for the dimer constituents [17]. Fig. 4 illustrates plots of calculated effective temperature versus the kinetic energy in the laboratory frame for KGGFL/YGGFL and YGGFL/VGGFL at high collision energy (50–200 eV). Note that fragment ion ratios at

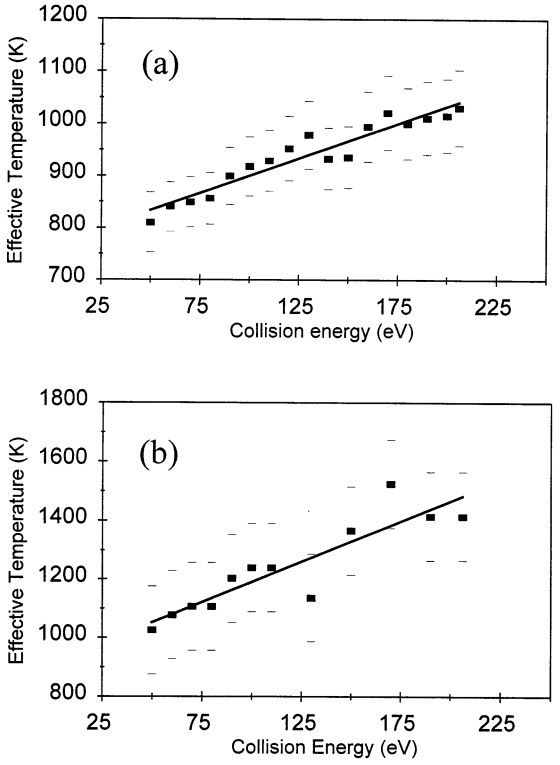

Fig. 4. The calculated effective temperature of proton-bound dimer composed of (a) YGGFL and KGGFL and (b) YGGFL and VGGFL vs. *KE* (lab) (eV). The error bars are estimated standard derivations of effective temperatures.

low collision energy (10–50 eV) are not considered because of their larger uncertainties and the limited number of data points. (There is an indication in the data for each of the systems of an abrupt change in partitioning behavior at ca. 45 eV collision energy indicative of two CID regimes. This effect might be indicative of a change in the CID mechanism.)

From the plots in Fig. 4, one can see that the effective temperatures for both the YGGFL/KGGFL and YGGFL/VGGFL dimers increase more or less linearly with *KE* in the collision energy range 50–200 eV. The effective temperature ranges from ca. 800–1000 K for YGGFL/KGGFL and from ca. 1000–1500 K for YGGFL/VGGFL. One can estimate the energy partitioning quotient for kinetic energy to internal energy conversion by utilizing Eq. (5), taking c as 0.3 instead of 0.2, to allow for a higher average effective temperature than that considered by Vékey, and taking the number of oscillators, s, as $3n - 6$. The value of 0.3 is also more consistent with the recent calculations of Drahos and Vékey [52]. At 1000 K they find c values of approximately 0.4 for a number of peptides. Table 2 includes the ΔGB's for the other cluster ion pairs estimated from literature data [34] as well as a summary of the energy partitioning results. The average estimated uncertainty for the partitioning quotient is around 15% of the value of the partitioning quotient. This is mainly because of uncertainties in the slopes ($\Delta T_{\text{eff}}/\Delta KE$) due, in turn, to uncertainties in the effective temperatures. An exception is the high estimated uncertainty $2 \pm 2\,\%$ for the partitioning quotient for VGGFL/GGGFL, that is a result of the larger scatter in the experimental fragment ion abundance ratios in this case. No consideration of the uncertainties in the factor $c(T, \nu)$ has been made. The results show that each of the systems displays a

Table 2
Energy partitioning information from CID of proton-bound dimers of pentapeptides

Pentapeptide	ΔGB[a] (eV)	E_{o1}[b] (eV)	E_{o2} (eV)	Energy partitioning quotient (%) (kinetic method)[c]	Energy partitioning quotient (%) (RRKM)
RGGFL/KGGFL	0.52	0.70	1.22	5 ± 1[d]	2 ± 1
KGGFL/YGGFL	0.30	1.12	1.42	2 ± 1	4 ± 1
YGGFL/VGGFL	0.03	1.36	1.39	3 ± 1	5 ± 1
VGGFL/GGGFL	0.08	1.32	1.40	2 ± 2	4 ± 3

[a]Calculated from [34] and [50] using $\Delta E_o = \Delta GB$.
[b]See text for estimates and comments on uncertainty.
[c]All data refer to lab collision energies (50–200 eV).
[d]"±" indicates uncertainty in energy partitioning quotient (%) without considering the uncertainty in ΔGB (see text).

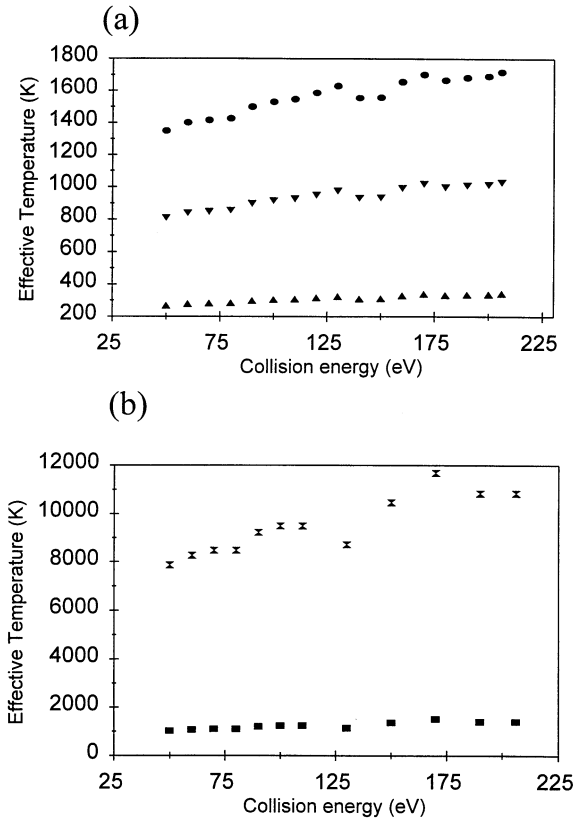

Fig. 5. Effect of uncertainties in ΔGB on the calculated effective temperature of proton-bound dimers composed of (a) YGGFL and KGGFL and (b) YGGFL and VGGFL vs. *KE* (lab) (eV). In (a) the inverted triangle indicates $\Delta GB = 0.30$ eV, the filled circle indicates $\Delta GB = 0.50$ eV, the triangle indicates $\Delta GB = 0.10$ eV. In (b) the filled square indicates $\Delta GB = 0.03$ eV, the hourglass indicates $\Delta GB = 0.23$ eV.

partitioning quotient of kinetic energy (lab) to internal energy that ranges from 2 % to 5 % (Table 2).

Note that the ΔGB values used in the kinetic method calculations are only approximate numbers and the calculated effective temperatures are strongly dependent on these values. This is the major weakness of the present study. Fig. 5(a) illustrates this dependence for KGGFL/YGGFL in the cases where ΔGB is allowed to range from 0.1 eV, 0.3 eV, and 0.5 eV. It can be seen that the slope ($\Delta T_{\text{eff}}/\Delta KE$) changes with ΔGB, and consequently, the calculated energy partitioning quotient changes from 3.3% ($\Delta GB = 0.5$ eV) to 0.7% ($\Delta GB = 0.1$ eV). The standard deviations associated with ΔGB are not known, however they are believed to be smaller than 0.2 eV, the value for which the effects have just been noted for KGGFL/YGGFL. For another dimer, YGGFL/VGGFL [Fig. 5(b)], the energy partitioning quotient ranges from 3 % ($\Delta GB = 0.03$ eV) to 23 % ($\Delta GB = 0.23$ eV) when this large range in ΔGB is allowed. These facts make it clear that the energy partitioning quotients obtained by this kinetic method approach are rough estimates only and that they depend on a knowledge of the difference in critical energies or, equivalently, ΔGB values. By contrast, they are much less strongly dependent on the actual values of the critical energies E_{o1} and E_{o2} (Table 2). The fact that these numbers are not well established is not of great significance to the present problem. Note too that the overall similarity in the energy partitioning behavior of the five peptide pairs studied constitutes evidence that the uncertainties in input thermochemical values do not preclude measurements to the level of accuracy claimed.

3.3. RRK calculations and estimation of kinetic energy to internal energy conversion

In an attempt to test the relationship between the effective temperature and the average internal energy [Eq. (3)] and to confirm the conclusions of the approximate treatment based on Eq. (3), the internal energy dependence of fragmentation was examined using RRK theory. According to RRK theory [53–56], the rate constant $k(E)$ at a given energy is:

$$k(E) = \nu[(E - E_o)/E]^{s-1} \quad (6)$$

where ν is the frequency factor, E is the internal energy, E_o is the critical energy for the reaction, and s is the effective number of degrees of freedom. Note that RRK theory may not be applicable to the dissociations of larger ions without modification [18, 57–59]. Based on previous studies using RRK theory [53–56], we take the effective number of degrees of freedom as $(3n - 6)/5$, where n is the total number of atoms in the proton-bound dimers of pentapeptides. It is widely recognized that RRK derived data fit experimental data best when the number of degrees of freedom is reduced by a factor of 3–5 from its original

defined value and that the reduction factors are themselves often energy dependent [60–65]. For the proton-bound dimer KGGFL–H^+–YGGFL, considering Eq. (1) and Eq. (6), we obtain the expression Eq. (7) on the assumption that the kinetic shift is negligible (but see RRKM discussion below) and that the frequency factor ν is the same for the two fragmentation pathways:

$$k_1(E)/k_2(E) = [(E - E_{o1})/(E - E_{o2})]^{[(3n-6)/5]} \quad (7)$$

Here E_{o1} is the critical energy for reaction 1 (producing $KGGFLH^+$) and E_{o2} is the critical energy for reaction 2 (producing $YGGFLH^+$). The difference in E_{o1} and E_{o2} can be taken as the difference in *GB*'s of the two constituent pentapeptides, provided the reverse activation energies are negligible, which is justifiable for simple bond cleavage of protonated dimers [34, 41, 66]. As discussed earlier, the difference in *GB*'s of the pentapeptides is assumed to be equal to the difference in PA's of the most basic residue in each pentapeptide. The larger critical energy, E_{o2}, is assumed to be 1.22 eV for the RGGFL/KGGFL ion. This value is an estimate based on the known binding energies for peptide clusters [10, 13–15, 67] (the thermal dissociations of peptide cluster ions also show similar activation energies [9, 11]). For example, the binding energies of proton-bound amino acid dimers were found to be in the range of 1.15 ± 0.05 eV [15]. The critical energies for the other systems are similarly estimated, based on their relative binding strengths or affinity values (see Table 2). For example, E_{o1} for producing $KGGFLH^+$ from the proton-bound dimer KGGFL/YGGFL is estimated as [GB(YGGFL)/GB(RGGFL)]*E_{o2} (critical energy for producing $KGGFLH^+$ from proton-bound dimers of RGGFL/KGGFL) ≈ [PA(tyrosine)/PA(arginine)]*E_{o2} (critical energy for producing $KGGFLH^+$ from proton-bound dimers of RGGFL/KGGFL). Fig. 6 shows a plot of fragment ion abundance ratios $[MH^+(KGGFL)]/[MH^+(YGGFL)]$ versus the internal energy *E* calculated by RRK theory. Comparing Fig. 6 and Fig. 3(a), one finds that the shapes of the curves are quite similar, in spite of the assumptions noted. One can obtain a plot of internal energy versus *KE*

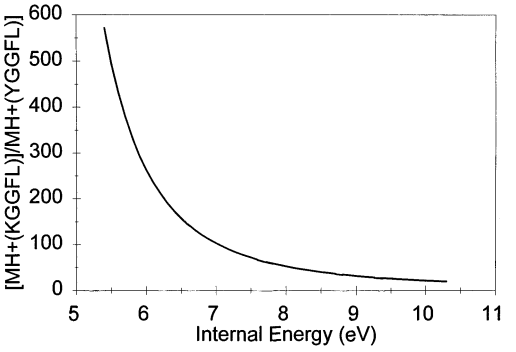

Fig. 6. Calculated fragment ion ratios $[MH^+(KGGFL)]/[MH^+(YGGFL)]$ vs. internal energy (eV) using RRK theory.

(lab) by combining the experimental branching ratio information of Fig. 3(a) with the calculated data of Fig. 6. Note that only data at higher collision energy (50–200 eV) are considered, for reasons stated previously. Good linear correlations between internal energy and *KE* are observed ($r = 0.959$) (Fig. 7). The slope of this plot, $\Delta E/\Delta KE$(lab), represents the average quotient for partitioning of kinetic energy to internal energy. This procedure is intended to correct for contributions of the initial internal energy before the collision, although the relative contribution of initial internal energy probably varies with a smaller proportion being contributed in the faster high collision energy regime. The estimated uncertainties in the partitioning factors are around 10% of their values. It

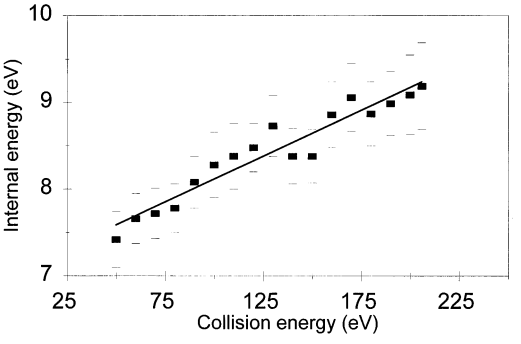

Fig. 7. Internal energy of proton-bound dimers of KGGFL/YGGFL calculated by RRK theory plotted against *KE* (lab). The error bars are estimated standard derivations in the internal energy associated with experimental standard deviations of fragment ion abundance ratios.

can be seen that the average energy partitioning quotient for this system is ~1%. The overall partitioning quotients range from 1% (KGGFL/YGGFL, VGGFL/GGGFL), 2% (YGGFL/VGGFL) to 3% (RGGFL/KGGFL). These results from the approximate RRK method encouraged further exploration of this approach using RRKM theory.

3.4. RRKM calculations and estimation of kinetic energy to internal energy conversion

The RRKM theory does not require the assumption regarding the frequency factor made in the RRK theory. It also does not involve the assumption of an "effective" number of degrees of freedom that is a significant weakness in RRK theory [60–65]. The rate constant is formulated as [68]:

$$k(E) = (\sigma/h)[W(E - E_o)/N(E)] \quad (8)$$

where $W(E - E_o)$ is the sum of the states in the transition state with $(E - E_o)$ internal energy, $N(E)$ is the density of states at E internal energy, σ is the reaction path degeneracy, and h is Planck's constant. $W(E - E_o)$ and $N(E)$ can be determined by a direct counting of states.

The RRKM calculations were performed by the "RRKM large" program described recently [69]. The program is capable of calculating reaction rates for large molecules (up to 1000 atoms) with large excess energy (up to 41 eV internal energy). The number of states is calculated by Beyer–Swinehart state counting, using no approximations. A "loose" transition state model and frequency set was used [69].

Fig. 8 shows plots of the calculated fragment ion abundance ratios, $[MH^+(KGGFL)]/[MH^+(YGGFL)]$ and $[MH^+(YGGFL)]/[MH^+(VGGFL)]$, versus internal energy. The shapes of the curves are similar to those obtained by experiment (Fig. 3). Note that the proton-bound dimers are assumed to have symmetrical structures with the proton bound between the two terminal amino-nitrogen atoms. This is likely to be the case for VGGFL/GGGFL and YGGFL/VGGFL, while for KGGFL/YGGFL and RGGFL/KGGFL, side chains of lysine or arginine are more likely to bind the proton since their side-chain nitrogen atoms are more basic than the N-terminus nitrogens. However, in the case of KGGFL/YGGFL, the RRKM calculations show that the changes in fragment ion abundance ratios $[MH^+(KGGFL)]/[MH^+(YGGFL)]$ are negligible when the two different binding structures are considered with the fixed transition state model; this is so even when the frequencies of the bonds other than those making up the dimer are varied over a range of ±20%. This is not unexpected since the side chain amino group is a similar primary amine to the N-terminus and the lysine residue is the residue closest to the N-terminus for KGGFL/YGGFL. In the case of RGGFL/KGGFL, the side chain-bound and N-terminus-bound structures are significantly different. With arginine, the expected side chain-protonated

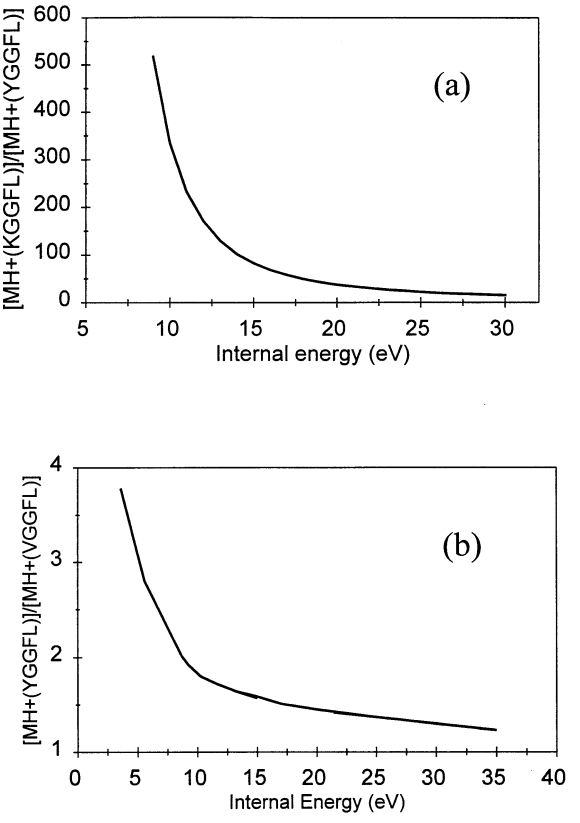

Fig. 8. Calculated fragment ion ratios (a) $[MH^+(KGGFL)]/[MH^+(YGGFL)]$ and (b) $[MH^+(YGGFL)]/[MH^+(VGGFL)]$ vs. internal energy (eV) using RRKM theory.

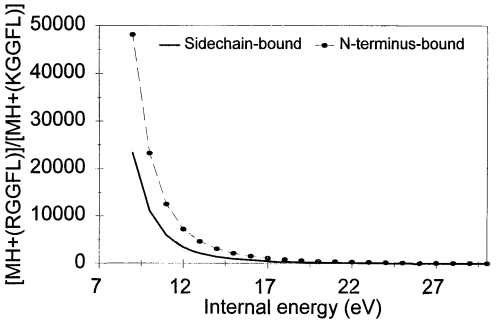

Fig. 9. Calculated fragment ion ratios $[MH^+(RGGFL)]/[MH^+(KGGFL)]$ vs. internal energy (eV) for two different structures of the proton-bound dimer (RRKM theory).

product ion is quite different from a normal primary immonium ion in that the positive charge is shared among three nitrogen atoms and a sp^2 carbon atom. The transition state models for these two structures are different. Fig. 9 illustrates the results of an RRKM calculation on RGGFL/KGGFL for two different structures of the proton-bound dimer. A pronounced decrease in fragment ion ratios $[MH^+(RGGFL)]/[MH^+(KGGFL)]$ is observed with the side chain-bound structure. We can not decide, definitively, between these two structures in this particular case. Consequently, the energy partitioning data will be affected by the structure of the proton-bound dimer. These effects are especially pronounced at low collision energy, where the uncertainties in experimental data are also greatest.

As was the case for the RRK calculations, one can obtain the total internal energy corresponding to a specific peak ratio from curves such as that shown in Fig. 8. Plots of internal energy versus *KE* (lab) can be made by using the fragment ion abundance ratios to connect the collision energies of Fig. 3 with the internal energies of Fig. 8. Good linear correlations between internal energy and *KE* (lab) are observed (Fig. 10). Note that the slope of the curve is of most interest since it represents a differential measurement that is largely insensitive to the precollision internal energy. The partitioning quotient (lab system) is ca. $4 \pm 1\%$ ($r = 0.963$) for YGGFL/KGGFL. Note that the critical energies used in these calculations are only approximate values and, as already noted, the calculated internal energies are strongly dependent on the *differences* in the values of the critical energies. Thus, the partitioning quotients must be considered as only approximate and the indicated uncertainties do not take this into account. As an illustration, Fig. 11 shows plots of calculated fragment ion ratios $[MH^+(KGGFL)]/[MH^+(YGGFL)]$ versus internal energy for a fixed difference in critical energies using the RRKM calculation. As expected, the peak ratios are insensitive to changes in critical energies as long as the difference in critical energies is fixed. The same observations also apply to the other systems studied. Thus, individual critical energy values (E_{o1} and E_{o2}) *do not* affect the energy partitioning quotient if the

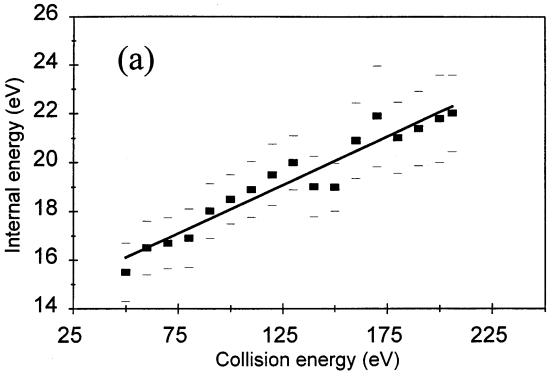

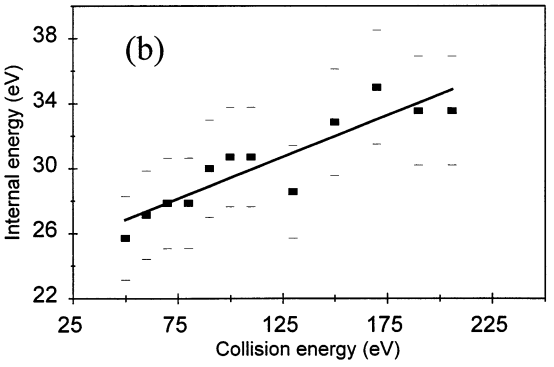

Fig. 10. Internal energies of proton-bound dimers of (a) KGGFL/YGGFL and (b) YGGFL/VGGFL calculated by RRKM theory plotted against *KE* (lab). The error bars are estimated standard derivations of internal energy associated with experimental standard deviations of fragment ion abundance ratios.

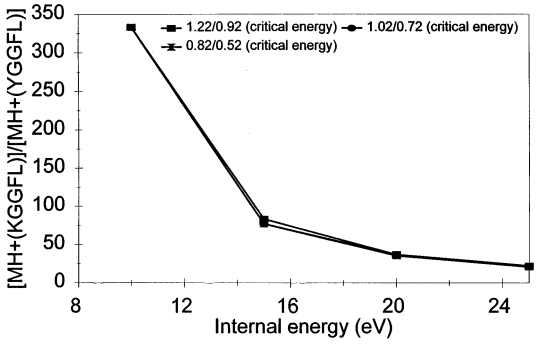

Fig. 11. Calculated fragment ion abundance ratios $[MH^+(KGGFL)]/[MH^+(YGGFL)]$ vs. internal energy (eV) at fixed $\Delta\varepsilon_o$ value ($\Delta\varepsilon_o$ = 0.30 eV) with different ε_{o1} and ε_{o2} values (RRKM theory).

difference in critical energy (ΔE_o) is fixed, i.e. ΔGB is fixed. However, when the difference in critical energies is changed, the behavior of peak ratios versus internal energy is also changed. Fig. 12 displays such a case for KGGFL/YGGFL where RRKM calculations are shown for a case in which the difference in critical energies is changed from 0.1–0.3 eV. The plots clearly show that the difference in critical energies is an important factor in evaluating the fragment ion ratio versus internal energy. Furthermore, the calculated results indicate that the difference in fragment ion ratios versus internal energy caused by differences in critical energies is minimized at high internal energy or low fragment ion ratios (corresponding to high collision energy). The internal

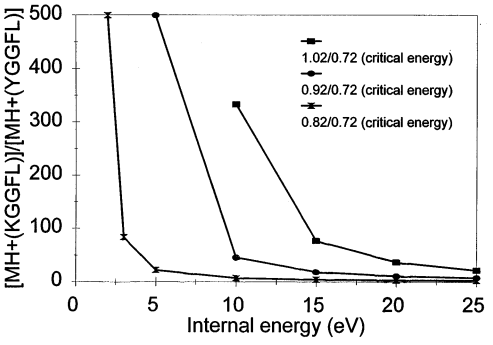

Fig. 12. Calculated fragment ion abundance ratios $[MH^+(KGGFL)]/[MH^+(YGGFL)]$ vs. internal energy (eV) for different $\Delta\varepsilon_o$ values (RRKM theory).

energy obtained from data at high collision energy is less sensitive to uncertainties in differences in critical energies. Thus, uncertainties in the differences in critical energies have a much larger impact on energy partitioning factors at low collision energy than at high collision energy. Again, this justifies the consideration of data only at high collision energy (>50 eV).

There are also other factors which impact on the method used to estimate internal energy. The first factor is the kinetic shift. It is well known that large biomolecules often exhibit large kinetic shifts during dissociation [69]. The kinetic shift varies as the square of the critical energy and is also dependent on the time scale [69]. For example, if the time scale is in the region of 1 to 10 ms, the kinetic shift is roughly equal to $6*E^2_{\text{critical}}$, i.e. 6 eV for a 1 eV critical energy. The uncertainty of critical energy estimated will lead to an uncertainty in kinetic shift. The nature of the present experiment, one in which kinetic energy is systematically varied, also dictates that the kinetic shift changes systematically with the collision energy. The estimation of internal energy of cluster ions by RRKM does not explicitly take into account the kinetic shift which is difficult to handle. Thus, the values are likely overestimated. The relative contribution of kinetic shift to the internal energy of cluster ions varies with collision energy and its impact on the accuracy of the estimated internal energy is likely to be significant at low collision energy. The second factor is the initial internal energy contribution from electrospray ionization, as stated previously. The exact initial internal energy distribution is not known, although the average value is estimated to be as high as 5 eV [12]. The procedure used in the calculation of energy partitioning (taking the slope of the internal energy versus collision energy curves) corrects substantially for the initial internal energy contribution. However, the relative contribution of initial internal energy probably varies with a larger proportion being made at low collision energy. Thus, data obtained from high collision energy are likely to be more reliable from the calculation point of view.

Table 2 includes calculated energy partitioning quotients using RRKM theory for each of the peptide

systems studied. It can be seen that the conversion quotients for the four pentapeptide cluster ions range from 2 % to 5 %. Note that the relatively larger uncertainty (~75 %) in the energy partitioning quotient associated with VGGFL/GGGFL is mainly caused by the scatter in the experimental fragment ion abundance ratios. The overall partitioning factors across the set of compounds are similar.

Collisional excitation in these systems might occur by one of two mechanisms, an impulsive mechanism or a collision complex mechanism. Impulsive mechanisms, i.e. an elastic collision between the target and part of the projectile ion with the center of mass energy for these collision partners being partitioned into vibration [18], have been suggested to play an important role in collision-induced dissociation over a wide range of conditions [6, 30, 58, 70, 71]. In the present case, the observed energy partitioning quotient is consistent with impulsive collisions. According to impulsive collision theory [58], the maximum amount of energy (Q_{max}) which can be transferred to internal energy can be calculated as:

$$Q_{max} = 4m_a m_{targ}^2 (m_{proj} - m_a) KE_{lab} / [(m_{targ} + m_a)^2 m_{proj}^2] \quad (9)$$

where m_a is the average atomic mass of the projectile ion, m_{proj} is the mass of the proton-bound peptide dimer and m_{targ} is the mass of target gas (Ar). When $m_a = 7$ [57], $m_{targ} = 40$, $m_{proj} = 1000$, the calculated (lab) energy partitioning quotient (Q_{max}/KE_{lab}) is around 2 % and when $m_a = 14$ the value approaches 4 %. The results are in the range of the experimental values (2 % to 5 %). The energy partitioning quotient is also consistent with the much less well characterized collision complex mechanism of activation. In this process there is almost quantitative transfer of the center of mass collision energy into internal energy. The present results show just such quantitative transfer (in typical cases, the center of mass energy is just 4 % of the laboratory collision energy) and as such are also consistent with a collision complex mechanism of activation in which the target atom is captured by the large biological molecular ion [28, 29].

4. Conclusions

Proton-bound dimers of pentapeptides, generated by electrospray ionization, were dissociated under single collision conditions over a range of energies. The collision energy dependence of the fragment ion abundance ratio was used to obtain the effective temperature of the activated cluster ions by the kinetic method. The effective temperatures obtained represent the internal energies of these activated proton-bound dimers. A combination of the kinetic method data and the relationship between internal energy and effective temperature [Eq. (3)], provides a rough estimate of the energy partitioning quotient for the conversion of kinetic energy to internal energy. These values lie in the range 2 % to 5 % for a collision energy range 50–200 eV. The energy partitioning behavior at low collision energy is not as well characterized because of the less accurate experiments (high ratios) and the larger effects of uncertainties in ΔGB and initial internal energies. The values found in this study are a little lower than those of McLuckey [41] for the proton-bound dimers of simple alkylamines.

On the assumption that the effective number of degrees of freedom is one-fifth of the total and that the difference in critical energies equals the difference in *GB*'s of pentapeptides, RRK calculations were performed in an independent attempt to estimate the total internal energy of the activated cluster ions. The shapes of the plots between k_1/k_2 versus *KE* (lab) (experimentally determined) and k_1/k_2 versus *E* (RRK calculation) are similar. By plotting the internal energy against *KE* (lab), one obtains the partitioning quotient from the slope. The partitioning quotients (lab) range from 1% to 3%. The preferred RRKM calculation was also performed to investigate the total internal energy of the activated cluster ions and the energy partitioning during CID. Similar partitioning factors to those obtained when working up the experimental data using the kinetic method were found by the RRKM calculation, values ranging from 2 % to 5 %. The data are subjected to significant uncertainties due to a lack of precise knowledge of thermochemical values (kinetic method) and difficulties in

treating kinetic shifts (RRKM). Nevertheless, the rough agreement between results from the kinetic method and those from RRKM calculations, and the agreement between data for the five different systems, provides some confidence in the conclusion that the 50–200 eV data are consistent with impulsive collisional activation. It is not possible to exclude a collision complex mechanism.

Although inaccuracies in the thermochemistry and the measurements may be responsible for the differences in the energy partitioning quotients for different systems, the possibility is not excluded that structural differences in the proton-bound dimers are responsible. Internal salt bridging [10, 13, 14, 17] may be responsible for differences in fragmentation behavior. It is possible that the BIRD technique may be suited for obtaining accurate thermochemical information on the present polypeptide systems. The methodology used in this study is expected to be applicable to other cluster ions involving biomolecules. With improvements in the theoretical treatments and more accurate thermochemical data, the combination of the kinetic method and RRKM calculation might provide an alternative way to obtain the important internal energy deposition information in CID of large cluster ion systems. This information might be useful in providing insights into the mechanism(s) by which collisional activation occurs.

Acknowledgements

The work at Purdue University was supported by the National Science Foundation, CHE 92-23791 and 9732670. The authors thank Dr. J.S. Patrick for providing synthetic peptides. G.C. acknowledges fellowship support from the National Science Foundation through the National Science Foundation/National Institute of Standards and Technology Graduate Student Research Program. Certain commercial equipment, instruments, or materials are identified in this report to specify adequately the experimental procedure. Such identification does not imply recommendation or endorsement by the National Institute of Standards and Technology, nor does it imply that the material or equipment identified are necessarily the best available for the purpose.

References

[1] C.M. Whitehouse, R.M. Dreyer, M. Yamashita, J.B. Fenn, Anal. Chem. 57 (1985) 675.
[2] K.R. Jennings, G.G. Dolnikowski, in J.A. McCloskey (Ed.), Mass Spectrometry, Methods in Enzymology, Academic, London, 1990, Vol. 193, pp. 37–61.
[3] M.M. Sheil, P.J. Derrick, Org. Mass Spectrom. 23 (1988) 429.
[4] M.M. Sheil, M. Guilhaus, P.J. Derrick, Org. Mass Spectrom. 25 (1990) 671.
[5] C.D. Bradley, P.J. Derrick, Org. Mass Spectrom. 26 (1991) 395.
[6] E. Uggerud, P.J. Derrick, Z. Naturforsch 44a (1989) 245.
[7] A.J. Alexander, P. Thibault, R.K. Boyd, J. Am. Chem. Soc. 112 (1990) 2484.
[8] D.L. Bricker, D.H. Russell, J. Am. Chem. Soc. 108 (1986) 6174.
[9] M. Busman, A.L. Rockwood, R.D. Smith, J. Phys. Chem. 96 (1992) 2397.
[10] R.A. Jockusch, P.D. Schnier, W.D. Price, E.F. Strittmatter, P.A. Demirev, E.R. Williams, Anal. Chem. 69 (1997) 1119.
[11] M. Meot-Ner (Mautner), A.R. Dongré, Á. Somogyi, V.H. Wysocki, Rapid Commun. Mass Spectrom. 9 (1995) 829.
[12] K. Vékey, Á. Somogyi, V.H. Wysocki, Rapid Commun. Mass Spectrom. 10 (1996) 911.
[13] W.D. Price, P.D. Schnier, E.R. Williams, Anal. Chem. 68 (1996) 859.
[14] P.D. Schnier, W.D. Price, R.A. Jockusch, E.R. Williams, J. Am. Chem. Soc. 118 (1996) 7178.
[15] W.D. Price, P.D. Schnier, E.R. Williams, J. Phys. Chem. 101 (1997) 664.
[16] S. Campbell, M.T. Rodgers, E.M. Marzluff, J.L. Beauchamp, J. Am. Chem. Soc. 117 (1995) 12840.
[17] W.D. Price, R.A. Jockusch, E.R. Williams, J. Am. Chem. Soc. 119 (1997) 11988.
[18] S.A. McLuckey, J. Am. Soc. Mass Spectrom. 3 (1992) 599.
[19] A.K. Shukla, J.H. Futrell, Mass Spectrom. Rev. 12 (1993) 211.
[20] S.A. McLuckey, R.G. Cooks, in F.W. McLafferty, Tandem Mass Spectrometry, Wiley, New York, 1983, p. 303.
[21] R.K. Boyd, E.E. Kingston, A.G. Brenton, J.H. Beynon, Proc. Roy. Soc. London (A) 392 (1984) 59.
[22] M.E. Bier, J.H. Amy, R.G. Cooks, J.E.P. Syka, P. Ceja, G. Stafford, Int. J. Mass Spectrom. Ion Processes 77 (1987) 31.
[23] J. Durup, in K. Ogata and T. Hayakawa (Eds.), Recent Developments in Mass Spectrometry, University of Tokyo Press, Tokyo, 1970, p. 921.
[24] V.H. Wysocki, H.I. Kenttämaa, R.G. Cooks, Int. J. Mass Spectrom. Ion Processes 75 (1987) 181.
[25] K.L. Schey, H.I. Kenttamaa, V.H. Wysocki, R.G. Cooks, Int. J. Mass Spectrom. Ion Processes 90 (1990) 71.

[26] K. Vékey, Á. Somogyi, V.H. Wysocki, J. Mass Spectrom. 30 (1995) 212.
[27] R.G. Cooks, L. Hendricks, J.H. Beynon, Org. Mass Spectrom. 10 (1975) 625.
[28] E.M. Marzluff, S. Campbell, M.T. Rodgers, J.L. Beauchamp, J. Am. Chem. Soc. 116 (1994) 7787.
[29] E.M. Marzluff, S. Campbell, M.T. Rodgers, J.L. Beauchamp, J. Am. Chem. Soc. 116 (1994) 6947.
[30] A.J. Alexander, R.K. Boyd, Int. J. Mass Spectrom. Ion Processes 90 (1989) 211.
[31] P. Thibault, A.J. Alexander, R.K. Boyd, J. Am. Soc. Mass Spectrom. 4 (1993) 835.
[32] P. Thibault, A.J. Alexander, R.K. Boyd, K.B. Tomer, J. Am. Soc. Mass Spectrom. 4 (1993) 845.
[33] R.G. Cooks, T.L. Kruger, J. Am. Chem. Soc. 99 (1979) 1279.
[34] R.G. Cooks, J.S. Patrick, T. Kotiaho, S.A. McLuckey, Mass Spectrom. Rev. 13 (1994) 287.
[35] R.G. Cooks, T.L. Kruger, J. Am. Chem. Soc. 101 (1981) 3274.
[36] S.A. McLuckey, D. Cameron, R.G. Cooks, J. Am. Chem. Soc. 103 (1981) 1313.
[37] L.G. Wright, S.A. McLuckey, R.G. Cooks, K.V. Wood, Int. J. Mass Spectrom. Ion Processes 42 (1982) 115.
[38] G. Boand, R. Houriet, T.J. Gaumann, J. Am. Chem. Soc. 105 (1983) 2203.
[39] J.S. Brodbelt, R.G. Cooks, Talanta 36 (1989) 255.
[40] K. Vékey, J. Mass Spectrom. 31 (1996) 445.
[41] S.A. McLuckey, Org. Mass Spectrom. 19 (1984) 545.
[42] M. Morris, D.E. Riederer Jr., B.E. Winger, R.G. Cooks, T. Ast, C.E.D. Chidsey, Int. J. Mass Spectrom. Ion Processes 122 (1992) 181.
[43] V.H. Wysocki, J.M. Ding, J.L. Jones, J.H. Callahan, F.L. King, J. Am. Soc. Mass Spectrom. 3 (1992) 29.
[44] S.A. Miller, D.E. Riederer Jr., R.G. Cooks, W.R. Cho, H.W. Lee, H. Kang, J. Phys. Chem. 98 (1994) 245.
[45] L.A. Horn, S.H. Hoke II, R.G. Cooks, unpublished results.
[46] H.N. Lee, J.L. Beauchamp, presented at the 209th National Meeting of the American Chemical Society, Anaheim, CA, April 2–7, 1995.
[47] S.L. Craig, M. Zhong, B. Choo, J.L. Brauman, J. Phys. Chem. A 101 (1997) 19.
[48] R.G. Cooks, A.L. Rockwood, Rapid Commun. Mass Spectrom. 5 (1991) 93.
[49] Z. Wu, C. Fenselau, Tetrahedron 49 (1993) 9197.
[50] S.A. McLuckey, R.G. Cooks, J.E. Fulford, Int. J. Mass Spectrom. Ion Phys. 52 (1983) 165.
[51] X. Cheng, Z. Wu, C. Fenselau, J. Am. Chem. Soc. 115 (1993) 4844.
[52] L. Drahos, K. Vekey, J. Am. Soc. Mass Spectrom. unpublished.
[53] Y.N. Lin, B.S. Rabinovitch, J. Phys. Chem. 74 (1970) 1769.
[54] P.F. Bente III, F.W. McLafferty, D.J. McAdoo, C. Lifshitz, J. Phys. Chem. 79 (1975) 713.
[55] D.J. McAdoo, P.F. Bente III, M.L. Gross, F.W. McLafferty, Org. Mass Spectrom. 9 (1974) 525.
[56] L.G. Lawrence, D.J. McAdoo, J. Am. Soc. Mass Spectrom. 4 (1993) 11.
[57] E.W. Schlag, R.D. Levine, Chem. Phys. Lett. 163 (1989) 523.
[58] E. Uggerud, P.J. Derrick, J. Phys. Chem. 95 (1991) 1430.
[59] P.J. Mckeown, M.V. Johnston, J. Am. Soc. Mass Spectrom. 2 (1991) 103.
[60] I. Howe, D.H. Williams, R.D. Bowen, Mass Spectrometry: Principles and Applications, 2nd Ed., McGraw-Hill, New York, 1981.
[61] R.G. Cooks, J.H. Beynon, R.M. Caprioli, G.R. Lester, Metastable Ions, Elsevier, New York, 1973.
[62] W.A. Chupka, J. Chem. Phys. 30 (1959) 191.
[63] A. Kropf, E.M. Eyring, A.L. Wahrhaftig, H. Eyring, J. Chem. Phys. 32 (1960) 149.
[64] B. Steiner, C.F. Giese, M.G. Inghram, J. Chem. Phys. 34 (1961) 189.
[65] K. Larsen, Fundamental Aspects of Organic Mass Spectrometry, Verlag Chemie, Weinheim, 1978.
[66] K.H. Lund, G. Bojesen, Int. J. Mass Spectrom. Ion Processes 156 (1996) 203.
[67] C.D. Bradley, P.J. Derrick, Org. Mass Spectrom. 28 (1993) 390.
[68] W. Forst, Theory of Unimolecular Reactions, Academic Press, New York, 1973.
[69] P.J. Derrick, P.M. Loyd, J.R. Christie, in I. Cornides, Gy. Horváth, K. Vékey (Eds.), Advances in Mass Spectrometry, Wiley, Chichester, 1995, Vol. 13, p. 23.
[70] R.G. Gilbert, M.M. Sheil, P.J. Derrick, Org. Mass Spectrom. 20 (1985) 430.
[71] G.M. Neumann, P.J. Derrick, Org. Mass Spectrom. 19 (1984) 165.